Parallels between the dynamics at the noise-perturbed onset of chaos in logistic maps and the dynamics of glass formation

F. Baldovin[1,2,3] and A. Robledo[1]

[1]*Instituto de Física, Universidad Nacional Autónoma de México, Apartado Postal 20-364, México 01000 D.F., Mexico*

[2]*INFM-Dipartimento di Fisica, Università di Padova, Via Marzolo 8, I-35131 Padova, Italy*

[3]*Sezione INFN, Università di Padova, Via Marzolo 8, I-35131 Padova, Italy*

(Received 1 April 2005; revised manuscript received 30 September 2005; published 22 December 2005)

We develop the characterization of the dynamics at the noise-perturbed edge of chaos in logistic maps in terms of the quantities normally used to describe glassy properties in structural glass formers. Following the recognition [Phys. Lett. A **328**, 467 (2004)] that the dynamics at this critical attractor exhibits analogies with that observed in thermal systems close to vitrification, we determine the modifications that take place with decreasing noise amplitude in ensemble- and time-averaged correlations and in diffusivity. We corroborate explicitly the occurrence of two-step relaxation, aging with its characteristic scaling property, and subdiffusion and arrest for this system. We also discuss features that appear to be specific to the map.

DOI: 10.1103/PhysRevE.72.066213 PACS number(s): 05.45.Ac, 05.40.Ca, 64.70.Pf

I. INTRODUCTION

The erratic motion of a Brownian particle is usually described by the Langevin theory [1]. As is well known, this method finds a way round the detailed consideration of many degrees of freedom by representing via a noise source the effect of collisions with molecules in the fluid in which the particle moves. The approach to thermal equilibrium is produced by random forces, and these are sufficient to determine dynamical correlations, diffusion, and a basic form for the fluctuation-dissipation theorem [1].

In the same spirit, attractors of nonlinear low-dimensional maps under the effect of external noise can be used to model states in systems with many degrees of freedom. In a one-dimensional map with only one control parameter μ the consideration of external noise could be thought to represent the effect of many other systems coupled to it, like in the so-called coupled map lattices [2]. Notice that the general map formula

$$x_{t+1} = x_t + h_\mu(x_t) + \sigma\xi_t \tag{1}$$

is a discrete form for a Langevin equation with nonlinear "friction force" term h_μ. In Eq. (1), $t=0,1,\ldots$ is the iteration time, ξ_t is a Gaussian white noise ($\langle\xi_t\xi_{t'}\rangle=\delta_{t,t'}$), and σ measures the noise intensity.

An interesting option offered by Eq. (1) is the study of singular states known to exhibit anomalous dynamics. For instance, the so-called onset of chaos in logistic maps is a critical attractor with nonergodic and nonmixing phase-space properties, and the perturbation of this attractor with noise transforms its trajectories into genuinely chaotic ones with regular ergodic and mixing properties. A case in point here would be to obtain the atypical dynamics near an ergodic to nonergodic transition and compare it, for example, to that in supercooled liquids close to glass formation, where also an ergodic to nonergodic transition is believed to occur. The dynamical properties for such glassy states appear associated with two-time correlations with loss of time translation invariance (TTI) and aging scaling properties, as well as with subdiffusion and arrest [3,4]. The specific question we would like to address is whether there are properties shared, and, if so, to what extent, by critical attractors in nonlinear low-dimensional maps and nonergodic states in systems with many degrees of freedom.

Recently [5], it has been realized that the dynamics at the noise-perturbed edge of chaos in logistic maps shows similarities with that observed in supercooled liquids close to vitrification. Three major features of glassy dynamics in structural glass formers—two-step relaxation, aging, and a relationship between relaxation time and configurational entropy—were shown to be displayed by the properties of orbits with vanishing Lyapunov coefficient. Interestingly, the previously known properties in control-parameter space of the noise-induced bifurcation gap (see Fig. 1) [6,7] play a central role in determining the characteristics of dynamical relaxation at the chaos threshold, and this was exploited to uncover the analogy between the dynamical and thermal systems in which the noise amplitude σ plays a role equivalent to a temperature difference $T-T_g$, where T_g is the so-called glass transition temperature [3,4].

In Ref. [5] only the properties of single-time functions (i.e., trajectories) were discussed and here we focus the analysis on two-time correlations. This would allow for a closer examination of the analogy with glassy dynamics as the study of the latter often centers on two-time correlations. However, we also look at diffusion properties via the determination of the mean-square displacement of trajectories in a suitably space-extended map. To lay emphasis on the similarities in the dynamics between the two types of systems we analyze the attainment of TTI in the correlations caused by the action of noise. We recall [8,9] that exposure of attractors to noise has the features of an activated process, a mechanism that is usually considered in the interpretation of relaxation processes in glass formers. Also we make up a simple "landscape" picture for the properties of the noise-perturbed map in order to compare it with that obtained from the multidimensional energy landscape of supercooled liquids. Aware of our crude attempt to contrast the dynamics of a

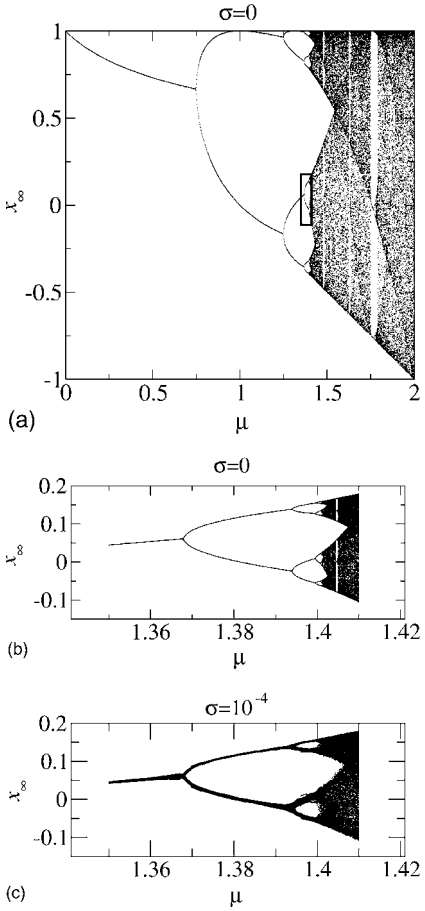

FIG. 1. (a) Logistic map attractor. (b) Magnification of the box in (a). (c) Noise-induced bifurcation gap in the magnified box.

single map (although equivalent to a coupled array of such maps when described via a Langevin-type equation) with that of thermal systems, we point out the main differences encountered. Specifically, the dynamics at the onset of chaos displays regular patterns absent in the known (experimental or computed) dynamics of molecular systems. These differences reflect the peculiarities of the period-doubling route to chaos displayed by unimodal maps.

The structure of the body of the article is as follows: In Sec. II we recall essential properties of the logistic map under additive noise—e.g., the bifurcation gap and its time-dependent manifestation at the chaos threshold. In Sec. III we present results on ensemble-averaged two-time correlations for $\sigma \gtrsim 0$, the attainment of TTI, and the development of two-step relaxation as $\sigma \to 0$. In Sec. IV we focus on time-averaged two-time correlations and the occurrence of the characteristic aging scaling at the onset of chaos with $\sigma=0$. In Sec. V we present a repeated-cell map for diffusion at the onset of chaos and show the evolution in behavior from diffusive to subdiffusive and finally to localization as $\sigma \to 0$. In Sec. VI we make final remarks.

II. NOISE-PERTURBED ONSET OF CHAOS

We describe now the effect of additive noise in the dynamics at the onset of chaos in the logistic map

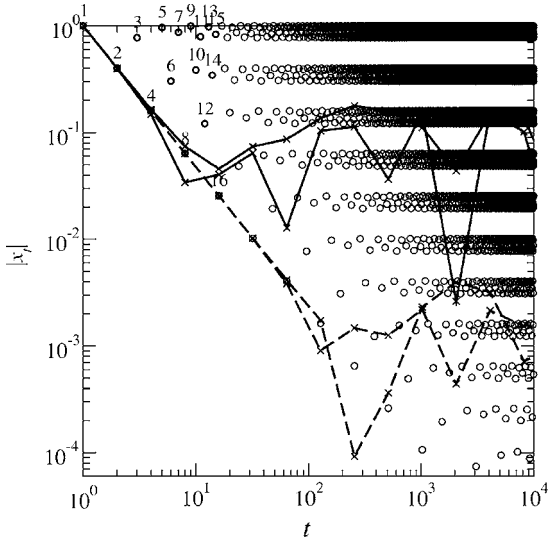

FIG. 2. Absolute values of positions in logarithmic scales of iterations t for various trajectories at the onset of chaos $\mu_c(\sigma)$ starting at $x_0=0$. Open circles correspond to $\sigma=0$ where the numbers label time $t=1,\ldots,16$. Solid (dashed) lines represent trajectories for noise amplitude $\sigma=10^{-3}$ ($\sigma=10^{-6}$) plotted only at times $t=2^n$.

$$x_{t+1} = 1 - \mu x_t^2 + \sigma \xi_t, \quad -1 \leqslant x_t \leqslant 1, \quad 0 \leqslant \mu \leqslant 2, \quad (2)$$

where h_μ in Eq. (1) has taken the form $h_\mu(x)=1-x-\mu x^2$. For $\sigma=0$ at the onset of chaos at $\mu_c=1.401\,15\ldots$ the orbit with attractor initial condition $x_0=0$ consists of positions arranged as nested power-law time subsequences that asymptotically reproduce the full period-doubling cascade that occurs for $\mu<\mu_c$ [10,11] (see the open circles in Fig. 2). This orbit is the last (the accumulation point) of the so-called "superstable" orbits of period 2^n which occur at $\mu=\bar{\mu}_n<\mu_c$, $n=1,2,\ldots$, a superstable orbit of period 2^∞. Superstable orbits include $x=0$ as one of their positions, and their Lyapunov exponent λ_1 diverges to $-\infty$ [6]. A transient dynamics at the onset of chaos is observed for trajectories with initial position outside the Feigenbaum attractor but we shall not consider this in what follows. For $\sigma>0$ the noise fluctuations wipe the fine structure of the periodic attractors as the iterate visits positions within a set of bands or segments similar to those in the chaotic attractors. Nevertheless, there remains a well-defined transition to chaos at $\mu_c(\sigma)$ where the Lyapunov exponent λ_1 changes sign [6,7]. The period doubling of bands ends at a finite maximum period $2^{N(\sigma)}$ as $\mu \to \mu_c(\sigma)$ [see Fig. 1(c)] and then decreases at the other side of the transition. This effect displays scaling features and is referred to as the bifurcation gap [6,7]. For instance, $\Delta\mu_c \sim \sigma^\gamma$ where $\Delta\mu \equiv \mu_c(0)-\mu_c(\sigma)$ and $\gamma=\ln \delta_F/\ln \nu$, where $\delta_F=0.466\,92\ldots$ is one of the two Feigenbaum's universal constants (the second, $\alpha_F=2.502\,90\ldots$, measures the power-law period-doubling spreading of iterate positions), and $\nu \simeq 2\sqrt{2}\alpha_F(1+1/\alpha_F^2)^{-1/2} \simeq 6.619$. See [5] and references therein. When σ is small the trajectories visit sequentially the set of $2^{N(\sigma)}$ disjoint bands leading to a cycle, but the behavior inside each band is irregular. These trajectories represent ergodic states as the accessible positions have a fractal dimen-

sion equal to the dimension of phase space. When $\sigma=0$ the trajectories correspond to a nonergodic state, since as $t\to\infty$ the positions form only a Cantor set of fractal dimension $d_f=0.538\ldots$. Thus the removal of the noise $\sigma\to 0$ leads to an ergodic-to-nonergodic transition in the map.

As shown in Ref. [5] when $\mu=\mu_c(\sigma)$ $(\sigma>0)$ there is a "crossover" or "relaxation" time $t_x=\sigma^{r-1}$, $r=1-\ln 2/\ln \nu \simeq 0.6332$, between two different time evolution regimes. This crossover occurs when the noise fluctuations begin suppressing the fine structure of the attractor as displayed by the superstable orbit with $x_0=0$ described above (see solid and dashed lines in Fig. 2). For $t<t_x$ the fluctuations are smaller than the distances between the neighboring subsequence positions of the $x_0=0$ orbit at $\mu_c(0)$, and the iterate position with $\sigma>0$ falls within a small band around the $\sigma=0$ position for that t. The bands for successive times do not overlap. The time evolution follows a subsequence pattern close to that in the noiseless case. When $t\sim t_x$ the width of the noise-generated band reached at time $t_x=2^{N(\sigma)}$ matches the distance between adjacent positions, and this implies a cutoff in the progress along the position subsequences. At longer times $t>t_x$ the orbits no longer trace the precise period-doubling structure of the attractor. The iterates now follow increasingly chaotic trajectories as bands merge with time. This is the dynamical image—observed along the time evolution for the orbits of a single state $\mu_c(\sigma)$—of the static bifurcation gap initially described in terms of the variation of the control parameter μ [7].

The entropy associated with the distribution of the iterate positions within the 2^N bands has the form $S_c=2^N\sigma s$, where s is the entropy associated with a single band. Use of $2^N=t_x$ and $t_x=\sigma^{r-1}$, $r-1\simeq -0.3668$ [5], leads to

$$t_x=(s/S_c)^{(1-r)/r}. \tag{3}$$

Since $(1-r)/r\simeq 0.5792$, then $t_x\to\infty$ and $S_c\to 0$ as $\sigma\to 0$. See [5] for details on the derivation. We have compared [5] this expression with its counterpart in structural glass formers: the Adam-Gibbs equation [3].

III. TWO-STEP RELAXATION

The time evolution of equilibrium two-time correlations in supercooled liquids on approach to glass formation display a two-step process of relaxation. This consists of a primary power-law decay in time difference $t=t_2-t_1$ that leads into a plateau, and at the end of this there is a second power-law decay that evolves into a faster decay that can be fitted by a stretched exponential [3]. Also, the duration t_x of the plateau increases as an inverse power law of the difference $T-T_g\gtrsim 0$ as the temperature T decreases to the glass transition temperature T_g. The first and second decays are usually referred to as the β and α relaxation processes, respectively [3]. An observable example of such a correlation function, both experimentally and numerically, is the Fourier transform of the density-density correlation at time difference t. The former is known as the intermediate scattering function while the latter is known as the van Hove function [3].

The study of single-trajectory properties (one time functions) in Ref. [5] led to the suggestion that the dynamical behavior in the map at $\mu_c(\sigma)$ would show parallels to the relaxation properties of glass formers. For instance, the analog of the β relaxation would be obtained by considering initial conditions x_0 outside the critical attractor since the ensuing orbits display a power-law transient as the positions approach asymptotically those of the attractor. The intermediate plateau would correspond to the regime $t<t_x$, described in the previous section, when the iterates are confined to nonintersecting bands before they reach the bifurcation gap; its duration t_x grows as an inverse power law of σ. The analog of the α relaxation was proposed to be the band-merging crossover process that takes place for $t>t_x$. To explore more closely these similarities we evaluated the two-time correlation function

$$c_e(t_1,t_2)=\frac{\langle x_{t_2}x_{t_1}\rangle-\langle x_{t_2}\rangle\langle x_{t_1}\rangle}{\chi_{t_1}\chi_{t_2}},\quad ,1\leqslant t_1\leqslant t_2, \tag{4}$$

for different values of the noise amplitude σ. In Eq. (4), $\langle\cdots\rangle$ represents an average over an ensemble of trajectories, all of them starting with initial conditions $x_0=0$ and $\chi_{t_i}=\sqrt{\langle x_{t_i}^2\rangle-\langle x_{t_i}\rangle^2}$.

We first address the question of whether the exposure of trajectories to noise has the effect of introducing, after an initial transient period, a time translation invariance property into the correlation in Eq. (4)—i.e., $c_e(t_1,t_2)\simeq c_e(t=t_2-t_1)$, t_1 large. The presence of this effect would be analogous to thermalization in molecular systems, after which equilibrium correlations are measured or computed (in glass forming systems for $T>T_g$). In Fig. 3 we show how TTI develops and is maintained for a sufficiently large time difference interval $t=t_2-t_1$. The numerical limitation in evaluating accurate values for $\mu_c(\sigma)$ leads to an upper bound for t, but we checked that increasing precision in $\mu_c(\sigma)$ leads to a larger interval for t for which TTI is observed. In view of the results shown in Fig. 3 we can conclude that under external noise of weak amplitude the ensemble of trajectories "thermalizes" asymptotically into an "equilibrium" attractor.

The TTI property in the map still retains certain memory of the initial t_1, only in a generic way that reflects the characteristic symmetries of the period-doubling onset of chaos of the logistic map. Notice that in Fig. 3 the values for t_1 are of the form $t_1=2^n+1$. It is found that both the initial decay and the value of the intermediate plateau of $c_e(t)$ are fixed when the values of t_1 belong to the sequence $t_1=2^n+k$, n large with k fixed. However the main decay process of $c_e(t)$ appears to be independent of t_1. In Figs. 4(a) and 4(b) we show the behavior of $c_e(t)$, respectively, when $t_1=2^n+1$ and $t_1=2^n-1$, $n=9,10,\ldots$. In the first case [Fig. 4(a)] the correlation maintains the initial value of unity from $t=0$ until the main decay process sets in, while in the second case [Fig. 4(b)] there is initial decay at short times followed by a plateau that ends when the same main decay as in Fig. 4(a) takes place. For other values of k the correlation $c_e(t)$ shows a behavior similar to that in Fig. 4(b) with different values for the duration of the initial decay (which we refer to as the β decay) and for the plateau, but always with the same main decay (which we refer to as the α decay). The α decay is

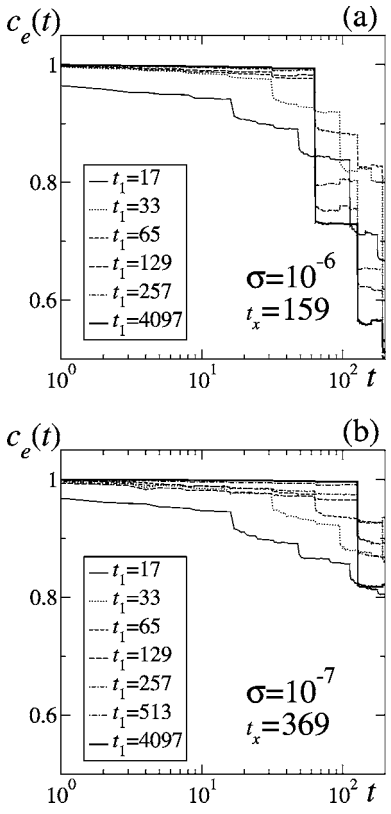

FIG. 3. Development of time translation invariance (TTI) in the correlation $c_e(t_1, t=t_2-t_1)$ through the action of noise of amplitude σ at the onset of chaos. All trajectories start $x_0=0$ and t_x is the time to reach the bifurcation gap.

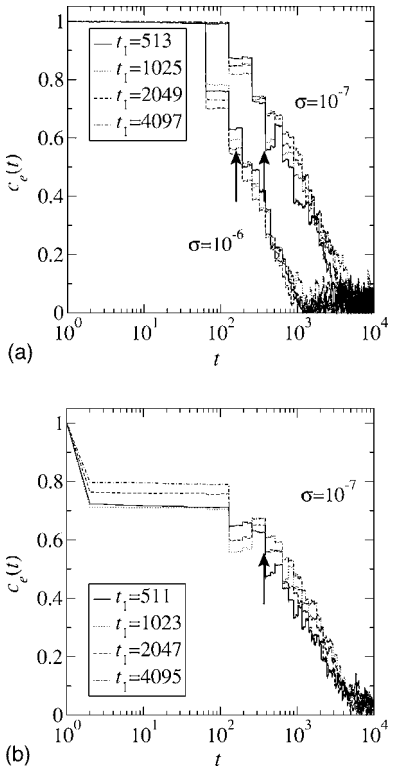

FIG. 4. Relaxation at the onset of chaos according to the correlation function $c_e(t_1, t=t_2-t_1)$ defined in Eq. (4) for an ensemble of 500 trajectories starting at $x_0=0$. In (a) t_1 is of the form 2^n+1 and the noise amplitude is $\sigma=10^{-6}$ and 10^{-7}. Vertical arrows, from left to right, indicate the crossover time $t_x(\sigma)$. In (b) $t_1=2^n-1$ and $\sigma=10^{-7}$.

itself made up of several plateaus the values of which alternate when n is varied [as shown in Figs. 4(a) and 4(b)]. In all cases the duration of the main plateau coincides approximatively with the crossover time t_x at which the bifurcation gap is reached [see the vertical arrows in Figs. 4(a) and 4(b)]. Thus, the identification of the encounter of the bifurcation gap as the triggering event of the α relaxation process [5] seems to be confirmed by the numerical evaluation of $c_e(t)$.

IV. AGING

In glass-forming systems when $T-T_g \lesssim 0$ (nonequilibrium) two-time correlations lose time translation invariance and the dependence on the two times t_1 and $t_2=t+t_1$ has the characteristic known as aging [4]. More specifically, the time scale for the response to an external perturbation increases with the waiting time t_w, the time interval $t_w=t_1-t_0$ from system preparation at $t_0=0$ to the moment of the perturbation at t_1. As a consequence, the equilibrium fluctuation-dissipation relation that relates response and correlation functions breaks down [4]. In this regime the decay of response and correlation functions displays a scaling dependence on the ratio t/t_w [4].

As indicated in Ref. [5] the power-law position subsequences shown in Fig. 2 that constitute the superstable orbit of period 2^∞ within the noiseless attractor at $\mu_c(0)$ imply a built-in aging scaling property for the single-time function x_t. These subsequences are relevant for the description of trajectories that are at first held at a given attractor position for a waiting period of time t_w and then released to the normal iterative procedure. We chose the holding positions to be any of those along the top band shown in Fig. 2 with $t_w=2k+1$, $k=0,1,\ldots$. One obtains [5]

$$x_{t+t_w} \simeq \exp_q(-\lambda_q t/t_w), \tag{5}$$

where $\exp_q(x) \equiv [1-(q-1)x]^{1/1-q}$ and $\lambda_q=\ln \alpha_F/\ln 2$. This property is gradually removed when noise is turned on. The presence of a bifurcation gap limits its range of validity to total times $t_w+t<t_x(\sigma)$ and so progressively disappears as σ is increased [5].

When $\sigma=0$ trajectories are nonergodic and ensemble and time averages are not equivalent. For this reason we use a time-averaged correlation $c(t_1,t_2)$ to study aging and its related scaling property at the onset of chaos for $\sigma=0$, instead of the ensemble-averaged $c_e(t_1,t_2)$ in Eq. (4). Also for this case $c_e(t_1,t_2)$ is not defined as $\chi_{t_i}=0$ when the initial positions are all $x_0=0$ or x_{t_w}. We chose for $c(t_1,t_2)$ the form

$$c(t_w, t+t_w) = (1/N)\sum_{n=n_0}^{N} \phi^{(n)}(t_w)\phi^{(n)}(t+t_w), \tag{6}$$

where $\phi(t)=f_{\mu_c}^{(t)}(0)$ and $f_\mu(x)=1-\mu x^2$ and with n_0 any positive integer and $N \gg n_0$ a large integer. This definition of

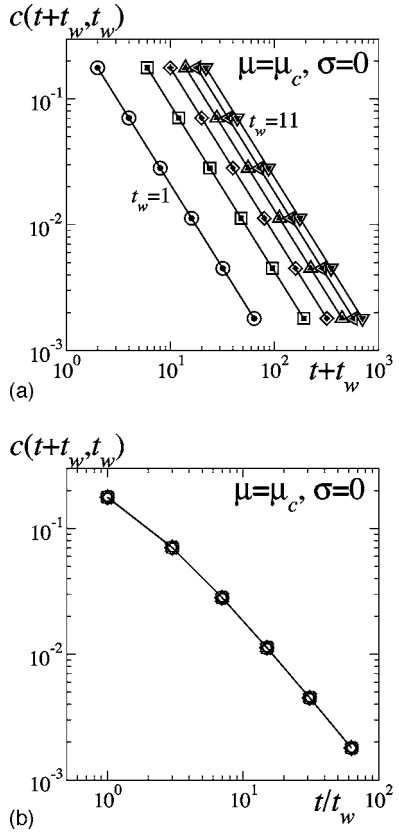

FIG. 5. Aging according to the correlation $c(t_w,t+t_w)$ given by Eq. (6) for the Feigenbaum attractor ($\mu=\mu_c$, $\sigma=0$). Total observation time is $n=1000$. In (a) is shown the explicit dependence on the waiting time (from left to right $t_w=1,3,5,7,9,11$). In (b) all curves collapse upon rescaling t/t_w.

$c(t_w,t+t_w)$ is designed to capture the power-law patterns of the trajectories at the noiseless onset of chaos. Equation (6) considers multiples of the two reference times t_w and $t+t_w$—i.e., times at which trajectories recurrently visit a given region of the attractor [15]. In Fig. 5(a) we show $c(t_w,t+t_w)$ for different values of t_w and in Fig. 5(b) the same data where the rescaled variable $t/t_w=2^n-1$, $t_w=2k+1$, $k=0,1,\ldots$, has been used. We have calculated $c(t_w,t+t_w)$ for different values of N and n_0 and found in both cases the same result as in Fig. 5(a). The characteristic scaling of aging behavior is especially clear.

V. SUBDIFFUSION AND ARREST

The sharp slowdown of dynamics in supercooled liquids on approach to vitrification is illustrated by the progression from normal diffusiveness to subdiffusive behavior and finally to a halt in the growth of the molecular mean-square displacement within a small range of temperatures or densities [12,13]. This deceleration of the dynamics is caused by the confinement of any given molecule by a "cage" formed by its neighbors, and it is the breakup and rearrangement of the cages which drives structural relaxation, letting molecules diffuse throughout the system. Evidence indicates that lifetime of the cages increases as conditions move toward the glass transition, probably because cage rearrangements involve a larger number of molecules as the glass transition is approached [12,13].

To investigate this aspect of vitrification in the map at $\mu_c(\sigma)$, we constructed a periodic map via repetition of a single (cell) map. This setting has being used to study deterministic diffusion in nonlinear maps, in which the trajectories migrate into neighboring cells due to chaotic motion. For fully chaotic maps diffusion is normal [6] but for marginally chaotic maps it is anomalous [14]. In our case we design the map in such a way that diffusion is due only to the random noise term; otherwise, motion is confined to a single cell. So we have the periodic map $x_{t+1}=F(x_t)$, $F(l+x)=l+F(x)$, $l=\ldots,-1,0,1,\ldots$, where

$$F(x)=\begin{cases}-|1-\mu_c x^2|+\sigma\xi, & -1\leqslant x<0,\\ |1-\mu_c x^2|+\sigma\xi, & 0\leqslant x<1.\end{cases} \tag{7}$$

Figure 6(a) shows the repeated-cell map together with a portion of one of its trajectories. As can be observed, the escape from the central cell into any of its neighbors occurs when $|F(x)|>1$ and this can only happen when $\sigma>0$. As $\sigma\to 0$ the escape positions are confined to values of x increasingly closer to $x=0$, and for $\sigma=0$ the iterate position is trapped within the cell. Likewise for any other cell. Figure 6(b) shows the mean-square displacement $\langle x_t^2\rangle-\langle x_t\rangle^2$ as obtained from an ensemble of trajectories initially distributed within the interval $[-1,1]$ for several values of noise amplitude. The progression from normal diffusion to subdiffusion and to final arrest can be plainly observed as $\sigma\to 0$. For small σ ($\leqslant 10^{-2}$), $\langle x_t^2\rangle-\langle x_t\rangle^2$ shows a downturn and later an upturn similar to those observed in colloidal glass experiments [12] and attributed to cage rearrangements. In the map this feature reflects cell crossings.

VI. FINAL REMARKS

As we have shown, the dynamics of logistic maps at the chaos threshold in the presence of noise displays elements reminiscent of glassy dynamics as observed in molecular glass formers. The limit of vanishing noise amplitude $\sigma\to 0$ (the counterpart of the limit $T-T_g\to 0$ in the supercooled liquid) leads to loss of ergodicity. This nonergodic state with vanishing Lyapunov coefficient $\lambda_1=0$ corresponds to the limiting state, $\sigma\to 0$, $t_x\to\infty$, of a family of small σ states with properties reminiscent of those in glass formers. Some additional comments may be useful to appreciate both similarities and differences between the two types of systems.

Activated dynamics is a standard component in understanding the relaxation mechanisms of glass formation [3,4], and so it is pertinent to note that there is a similar characteristic in the dynamics that we studied here. It has long been known [8,9] that the addition of external noise to a dissipative dynamical system (here a nonlinear one-dimensional map) causes its trajectories to escape from attractors. For chaotic attractors the mean escape time T has an exponential Arrhenius form

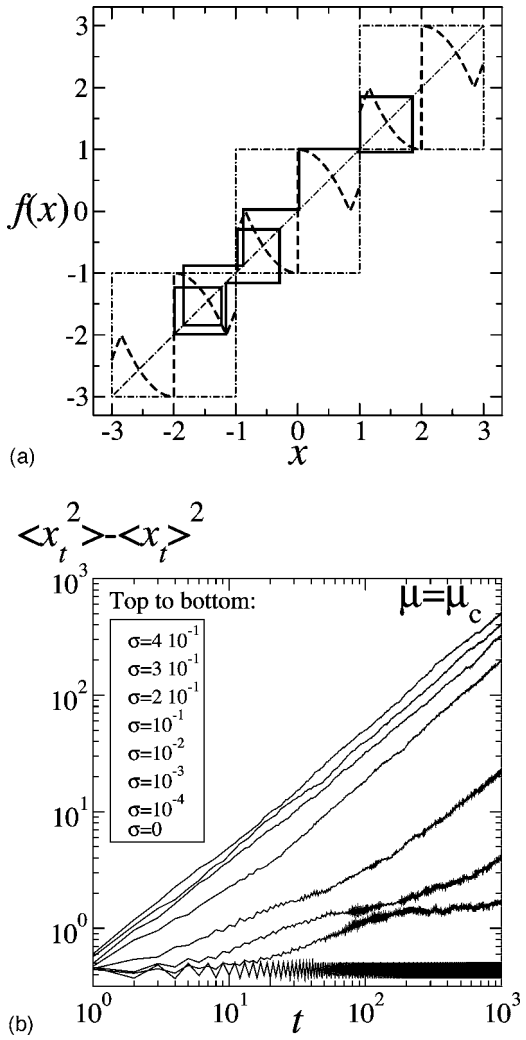

FIG. 6. Glassy diffusion in the noise-perturbed logistic map. (a) Repeated-cell map (thick dashed line) and trajectory (solid line). (b) Time evolution of the mean-square displacement $\langle x_t^2\rangle - \langle x_t\rangle^2$ for an ensemble of 1000 trajectories with initial conditions randomly distributed inside $[-1,1]$. Curves are labeled by the value of the noise amplitude.

$$T \approx T_0 \exp(E_0/R),$$

where E_0 and R are the minimum escape "energy" and noise "temperature," respectively, and T_0 is the inverse of the attempt rate. The difference from the usual molecular setup is that the escape is from the noiseless attractor and not from a minimum in the potential energy. For critical attractors, like the onset of chaos, the minimum escape energy vanishes and the escape time is expected to follow a power law with strong fluctuations [8,15]. We have seen that as $\sigma \to 0$ an increasing number of distinct but small phase-space bands are involved in an increasingly slow decay of dynamic correlations. On the other hand, in the usual picture of activated dynamics in glass formers the increase of the relaxation time as $T - T_g \to 0$ is thought to be associated with an increase in the landscape energy barriers and the assumption of some form of cooperative behavior by means of which a large number of particles are rearranged through a very slow process [3].

The structure of the phase-space regions that are sampled by trajectories as a function of the noise amplitude resemble the manner in which a glass-forming system samples its energy landscape as a function of temperature [3]. The numbers and widths of the attractor bands at noise amplitude σ can be thought to correspond to the numbers and extents of potential energy basins of the landscape at a given depth set by the temperature T. The "landscape" for the attractor has certainly a very simple structure when compared to that of the multidimensional energy landscape in a molecular system. At $\sigma = 0$ there is an infinite set of minima that consists of all the points $M \to \infty$ of the attractor, and as σ increases these minima merge into finite sets of $M = 2^{N(\sigma)}$ bands with N decreasing as σ grows. The regular merging by 2 in the numbers M and the features in the dynamics that they imprint are properties specific of logistic type maps. Other kinds of critical multifractal attractors, such as those for the critical circle map [6], would exhibit other properties characteristic of the route to chaos involved. This availability of detail would not be generally present in the measurements or numerical computation of the dynamics of a glass-forming molecular system.

It is of interest to note that at $\mu_c(\sigma)$ the trajectories and its resultant sensitivity to initial conditions are expressed for $t < t_x$ via the q exponentials of the Tsallis q statistics [5]. For $\sigma = 0$ these analytical forms are exact [10,15] and an identity linking accordingly generalized Lyapunov coefficients and rates of entropy production holds rigorously [11,15]. There is nonuniform convergence related to the limits $\sigma \to 0$ and $t \to \infty$. If $\sigma \to 0$ is taken before $t \to \infty$, orbits originating within the attractor remain there and exhibit fully developed aging properties, whereas if $t \to \infty$ is taken before $\sigma \to 0$, a chaotic orbit with exponential sensitivity to initial conditions would be observed.

ACKNOWLEDGMENTS

F.B. kindly acknowledges hospitality at UNAM where part of this work has been done. Work partially supported by DGAPA-UNAM and CONACyT (Mexican Agencies).

[1] See, for example, P. M. Chaikin and T. C. Lubensky, *Principles of Condensed Matter Physics* (Cambridge University Press, Cambridge, UK, 1995).

[2] K. Kaneko, Chaos **2**, 279 (1992).

[3] For a brief review see P. G. De Benedetti and F. H. Stillinger, Nature (London) **410**, 259 (2001).

[4] See also, C. A. Angell, K. L. Ngai, G. B. McKenna, P. F. McMillan, and S. W. Martin, J. Appl. Phys. **88**, 3113 (2000).

[5] A. Robledo, Phys. Lett. A **328**, 467 (2004); Physica A **342**, 104 (2004).
[6] See, for example, H. G. Schuster, *Deterministic Chaos. An Introduction*, 2nd revised ed. (VCH, Weinheim, 1988).
[7] J. P. Crutchfield, J. D. Farmer, and B. A. Huberman, Phys. Rep. **92**, 45 (1982).
[8] P. D. Beale, Phys. Rev. A **40**, 3998 (1989).
[9] P. Grassberger, J. Phys. A **22**, 3283 (1989).
[10] F. Baldovin and A. Robledo, Phys. Rev. E **66**, 045104(R) (2002).
[11] F. Baldovin and A. Robledo, Phys. Rev. E **69**, 045202(R) (2004).
[12] E. R. Weeks and D. A. Weitz, Chem. Phys. **284**, 361 (2002); Phys. Rev. Lett. **89**, 095704 (2002).
[13] A. Lawlor, D. Reagan, G. D. McCullagh, P. De Gregorio, P. Tartaglia, and K. A. Dawson, Phys. Rev. Lett. **89**, 245503 (2002).
[14] E. Barkai, Phys. Rev. Lett. **90**, 104101 (2003).
[15] E. Mayoral and A. Robledo, Phys. Rev. E **72**, 026209 (2005).